JACS
JOURNAL OF THE AMERICAN CHEMICAL SOCIETY

COMMUNICATION

pubs.acs.org/JACS

Thermodynamically Controlled Synthesis of a Chiral Tetra-cavitand Nanocapsule and Mechanism of Enantiomerization.

Junling Sun, James L. Bennett, Thomas J. Emge, and Ralf Warmuth*

Department of Chemistry and Chemical Biology, Rutgers. The State University of New Jersey, Piscataway, New Jersey 08854, United States

Supporting Information

ABSTRACT: The dynamic covalent synthesis, structure and conformational dynamics of a chiral polyimine nanocapsule **1a** are reported. Reaction of four tetraformyl cavitands and eight $H_2N(CH_2)_2NH_2$ yields quantitatively **1a**, which has a compact, asymmetrically folded, *pseudo*-C_2-symmetric structure, as determined by X-ray crystallography, and encapsulates four $CHCl_3$ and three CH_3OH guests in the solid state. In solution, **1a** enantiomerizes by passing over a barrier of $\Delta G_{298}^{\ddagger} = 21.5 \pm 0.7$ kcal mol^{-1} via a refolding process.

Investigation of reactivity and binding phenomena in the inner spaces of molecular capsules has moved the area of molecular encapsulation to a new level.[1] Nanosized molecular capsules have proven to be exceptional for stabilizing fleeting reactive intermediates,[2] accelerating,[3] or changing regiochemistry and product distribution of reactions,[3b,4] and exploring long-range electron- and energy-transfer processes.[5] For many applications of nanocapsules, chirality of the inner space would be a very valuable property and may result from using chiral building blocks or guests,[6] asymmetric arrangements of achiral building blocks,[7] or an asymmetric fold.[8] Here, we describe the thermodynamically controlled synthesis, structure, and dynamic properties of chiral nanocapsules **1a,b**, which assemble quantitatively from four tetraformylcavitands **2a,b** and eight 1,2-ethylenediamines **3**.

In earlier work, we reported the [6 + 12] polyimine nanocapsule **4a** that formed in 80% yield together with small amounts of the [4 + 8] nanocapsule **5a** upon reacting cavitand **6a** with two equivalents of ethylene-1,2-diamine.[9] Our motivation to test cavitand **2a** in similar multicomponent reactions came from the fact that **2a** can adopt a C_{4h}-symmetric structure, in which opposite aryl planes have angles close to 90°.[10] This would make **2a** an ideal building block for a multicomponent octahedral nanocapsule synthesis, if reacted with two equivalents of a linear diamine. We were then surprised, that the CF_3COOH-catalyzed condensation of **2a** with two equivalents of **3** did not yield the predicted [6 + 12] capsule, but instead gave quantitatively a [4 + 8]-condensation product **1a** based on GPC (see Supporting Information (SI)), NMR spectroscopy, and mass spectrometry. For example, the MALDI-TOF of **1a** showed the $[\mathbf{1a} + H]^+$ peak at the expected mass-to-charge ratio $m/z = 4358.72$ (calc.: $m/z = 4358.93$). The high efficiency of this synthesis results from the reversibility of the imine bond, which allows for error corrections during the capsule assembly.[11] The structure of **1a** was determined by X-ray crystallography and it was confirmed that **1a** has the same linker−cavitand connectivity as in **5a** and is very compact and asymmetrically folded (Chart 1 and Figure 1).[12]

Chart 1. Polyimine Nanocapsules 1, 4 and 5 and Cavitands 2 and 6

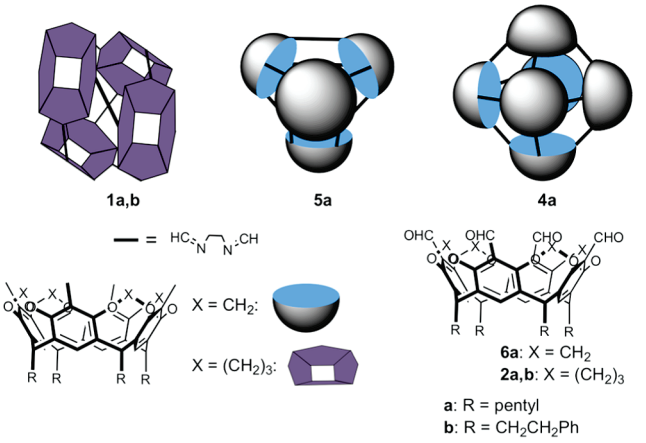

Nanocapsule **1a** crystallized from $CHCl_3/CH_3OH$ as pair of enantiomers in the unit cell, each having approximately C_2 symmetry and being filled with three $CHCl_3$ and three CH_3OH guest molecules. If viewed along the *pseudo*-C_2 axis, **1a** is nearly circular (Figure 1A) and has a U-shape, if viewed perpendicularly to this axis (Figure 1B). The connectivity in **1a** is identical to that in **5a**: Symmetry-related cavitands (two pairs colored in orange and purple) are singly linked, and one of the cavitands in each pair is doubly and singly linked to the cavitands in the other pair. In one pair of symmetry-related cavitands (colored in purple), the cavitands have a more flattened-out shape with their *pseudo*-C_2 axis passing through the center of the cavity of **1a**. The *pseudo*-C_2 axes of the other two cavitands (colored in orange) are almost parallel to the host's *pseudo*-C_2 axis. These cavitands are slightly shifted against each other and form multiple C−H-π and van der Waals interactions at the cavitand−cavitand interface involving spanner methylene groups of one cavitand and the aryl unit of the other cavitand. We believe that these interactions are important for the stability of this fold in solution (vide infra). The arrangement

Received: November 24, 2010
Published: February 18, 2011

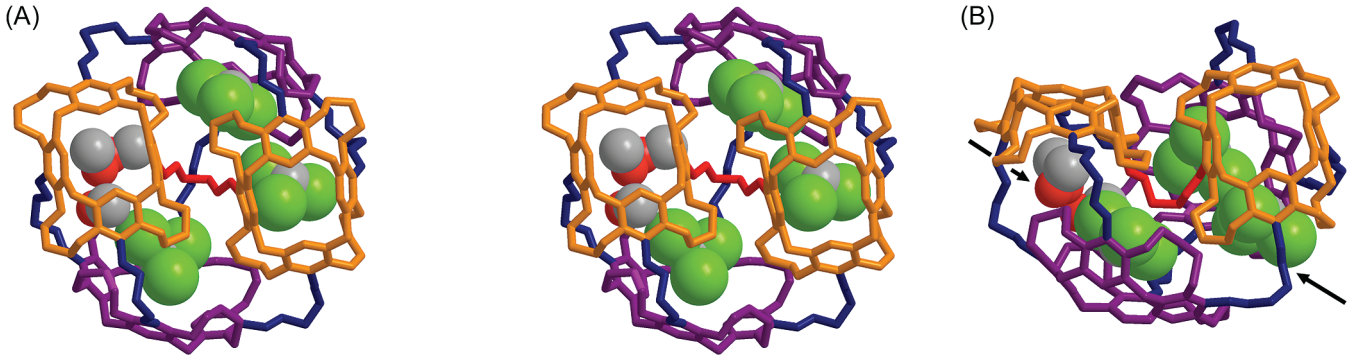

Figure 1. Stereo view of a tube model of the X-ray structure of nanocapsule **1a**⊙$[CHCl_3]_3[CH_3OH]_3$ along the *pseudo*-C_2 to axis (A) and view perpendicular to it (B). Appending pentyl groups, hydrogen atoms, and second component of disordered groups are omitted for clarity. Solvent molecules inside the cavity of **1a** are shown as space-filling models. Pairs of symmetry-related cavitands are colored in purple and orange. CH═N−CH_2CH_2−N═CH linkers are colored blue and red. Openings to the two cavities of **1a** are marked with arrows in (B).

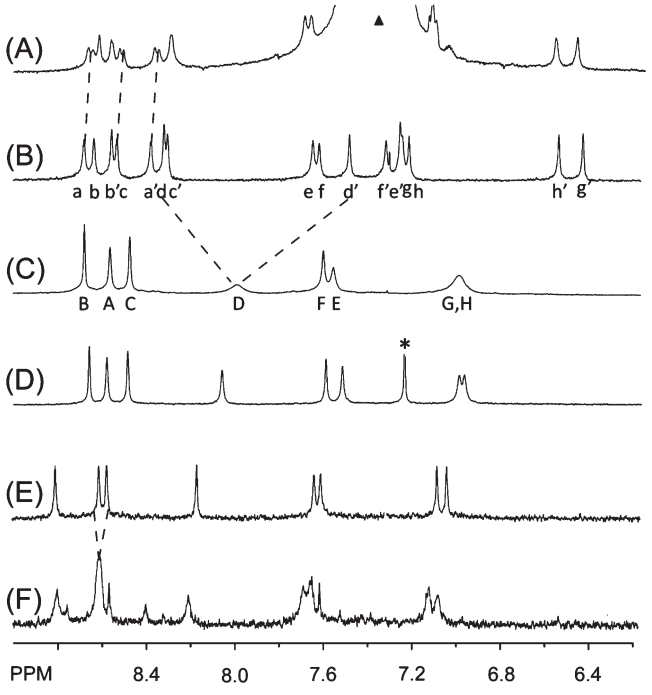

Figure 2. Partial ^{1}H NMR spectra (400 MHz) of **1a** showing the imine and aryl proton region of the spectrum. At −30 °C in CD_2Cl_2 + 2.7% (v/v) (−)-(*S*)-1-phenylethanol (A) and in CD_2Cl_2 (B). At 60 °C in CD_2Cl_2 (C), $CDCl_3$ (D) and $CDCl_2CDCl_2$ (E). At 110 °C in $CDCl_2CDCl_2$ (F). Signals assigned to imine and aryl protons of **1a**, $CHCl_3$ and (−)-(*S*)-1-phenylethanol are marked with letters a−d, e−h, asterisk, and filled triangle, respectively.

of the two orange-colored cavitands forces the linker that connects both cavitands (colored red in Figure 1) to fold toward the center of the host. This divides the host interior into two tube-shaped chambers, of which the right is filled with two $CHCl_3$ and the left with one $CHCl_3$ and three CH_3OH guests.

The low-temperature ^{1}H NMR spectrum of **1a** is consistent with the solid-state structure and suggests that **1a** is similarly folded in solution and has C_2 symmetry. At −30 °C, eight imine protons H_{im} and eight aryl proton H_a singlets, each in a ratio 2:2:2:2:2:2:2:2, are observed between 6.9 and 8.8 ppm (Figure 2B). Addition of 2.7% v/v of (−)-(*S*)-1-phenylethanol to this NMR solution led to splitting of several imine and aryl protons (Figure 2A), confirming the chirality of **1a**. Surprisingly, a screen of nine chiral, aromatic additives, of which several are structurally very similar to (*S*)-1-phenylethanol, such as (S)-α-methyl-2-pyridine methanol, failed to induce host signal splitting (see Figure S-21 in SI for structures). Presumably, these additives do not bind to **1a**.

Insight into the conformational stability of **1a** and rate of enantiomerization is important for chiral resolution and possible solution-phase applications of **1a**. Thus, we analyzed the dynamics of **1a** by 2D-EXSY spectroscopy and NMR line-shape analysis and identified two dynamic processes. The first process **I**, which has an activation free energy $\Delta G_{298}^{\ddagger}$ = 14.5 ± 0.4 kcal mol^{-1} ($\Delta H^{\ddagger}$ = 16.5 ± 0.2 kcal mol^{-1}; $\Delta S^{\ddagger}$ = 6.4 ± 0.7 cal mol^{-1} K^{-1}), leads to coalescence of pairs of imine and aryl protons, such that four imine and four aryl protons, each in a ratio 4:4:4:4, are observed at 60 °C (Figure 2C). Overall, the configuration of **1a** remains unchanged,[13] but the two symmetry-related cavitand pairs switch their position via reorganization of the structure, shown in a simplified way in Figure 3. The time-averaged structure of **1a** at this temperature has D_2-symmetry (D_2-**1a**). Upon warming the NMR sample to 110 °C, one pair of imine signals coalesced into a single signal (Figure 2E,F). Rapid exchange between protons in the remaining pairs of imine and aryl protons was confirmed by EXSY. This second process **II** leads to the enantiomerization of **1a** and has an activation free energy $\Delta G_{298}^{\ddagger}$ = 21.5 ± 0.7 kcal mol^{-1} ($\Delta H^{\ddagger}$ = 25.9 ± 0.4 kcal mol^{-1}; $\Delta S^{\ddagger}$ = 14.8 ± 1.1 cal mol^{-1} K^{-1}). Enantiomerization can be brought about by simple counterclockwise rotation of all cavitands in D_2-**1a**′ via achiral D_{2d}-**1a**, which would be a suitable time-averaged representation of **1a** at high temperature, followed by folding into C_2-**1a** (see top three structures in Figure 3).

Model examinations suggest that many contacts that are observed in the X-ray structure are lost during the repositioning and reorganization of the cavitands during the enantiomerization. Due to the high flexibility of spanners and bis-imine linkages of **1a** and its fairly compact fold, we believe that ground-state effects of this type contribute substantially to the barrier height rather than steric or angle/torsional strain effects in the transition state, which differs from most atropisomers,[14] but is consistent with observations in compact, twisted container molecules.[15] The configurational stability of **1a** should be sensitive to cavitand

dx.doi.org/10.1021/ja110475w |*J. Am. Chem. Soc.* 2011, 133, 3268–3271

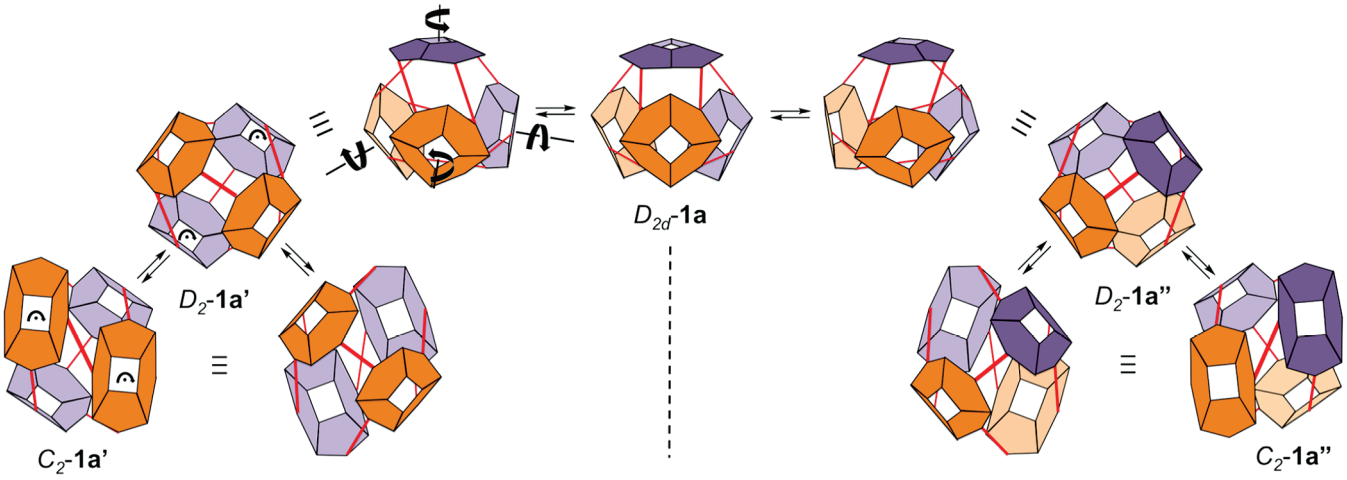

Figure 3. Schematic representation of the two nanocapsule refolding processes observed by NMR spectroscopy. In the low-temperature process **I**, C_2-**1a**′ is converted into itself via chiral D_2-**1a**′. In this refolding process, one pair of symmetry-related cavitands (pair I: orange) adopts the conformation and orientation of the cavitands in the second pair (pair II: purple) and vice versa. Refolding involves an initial clockwise rotation and outward tilting of pair I leading to D_2-**1a**′, followed by the exact reverse movements of cavitand pair II. The high-temperature process **II** leads to enantiomerization of **1a**′ and involves simultaneous counter-clockwise rotation of all cavitands in D_2-**1a**′ leading to its mirror image D_2-**1a**″, which further collapses into C_2-**1a**″. The labels **1a**′ and **1a**″ are used to differentiate the two enantiomers of **1a**.

Table 1. Enantiomerization Barrier $\Delta G_{323}^{\ddagger}$ of Nanocapsules 1a,b

solvent	$\Delta G_{323}^{\ddagger}$ (**1a**)/kcal mol^{-1}	$\Delta G_{323}^{\ddagger}$ (**1b**)/kcal mol^{-1}
CD_2Cl_2	n.d.[a]	21.1
$CDCl_3$	21.7	21
$CDCl_2CDCl_2$	21.1	20.6

[a] Signal broadening prevented EXSY experiments.

feet, solvent, and nature of the encapsulated guest(s), and should respond to the presence of acid and water or primary amines, which should destabilize **1** by promoting temporary breakage of imine bonds. Indeed, substitution of the pentyl feet with phenethyl feet lowered the barrier by approximately 0.5 kcal mol^{-1} (Table 1). Likewise, $\Delta G_{323}^{\ddagger}$ increases with the decreasing size of the solvent in the order $CDCl_2CDCl_2 < CDCl_3 < CD_2Cl_2$. Even though the overall change of $\Delta G_{323}^{\ddagger}$ is small, the data in Table 1 suggest that smaller feet and smaller guests allow **1a,b** to adapt a more compact and stable ground-state structure. Consistent with this interpretation are the large solvent-induced shifts (SIS) of imine and cavitand aryl proton resonances in the NMR spectrum of **1a** upon changing the solvent from CD_2Cl_2 or $CDCl_3$ to $CDCl_2CDCl_2$ (SIS_{max} = 0.18 ppm; Figure 2C−E). These SIS are difficult to explain with solvation effects and imply a small structural reorganization as encapsulated CD_2Cl_2 or $CDCl_3$ is replaced with the bulkier $CDCl_2CDCl_2$.

In summary, we have demonstrated a highly efficient synthesis of an asymmetrically folded tetracavitand nanocapsule **1** from 12 achiral building blocks. Considering the flexibility of the building blocks, **1** has a substantial enantiomerization barrier, which responds to changes in the cavitand feet and the size of the solvent. Current efforts in our laboratory are directed toward further increasing the configurational stability of **1** by fine-tuning the steric requirements and polarity of the appending feet and toward enantiomerically enriching **1**, which would be prerequisites for its application in chiral recognition and asymmetric synthesis.

■ ASSOCIATED CONTENT

Supporting Information. Experimental procedures, spectroscopic data, GPC trace, EXSY spectra, ^{1}H NMR spectra of **1a** at different temperatures and line-shape analysis, tables with rate constants, Eyring plots; CIF for **1a**. This material is available free of charge via the Internet at http://pubs.acs.org.

■ AUTHOR INFORMATION

Corresponding Author
warmuth@rutgers.edu

■ ACKNOWLEDGMENT

We warmly thank the National Science Foundation for financial support of this work (Grants CHE-0518351 and CHE-0957611).

■ REFERENCES

(1) (a) Cram, D. J.; Cram, J. M. *Container Molecules and Their Guests*; The Royal Society of Chemistry: London, 1994. (b) Koblenz, T. S.; Wassenaar, J.; Reek, J. N. H. *Chem. Soc. Rev.* **2008**, *37*, 247–262. (c) Pluth, M. D.; Bergman, R. G.; Raymond, K. N. *Acc. Chem. Res.* **2009**, *42*, 1650–1659. (d) Rebek, J. *Acc. Chem. Res.* **2009**, *42*, 1660–1668.(e) Warmuth, R. In *Molecular Encapsulation*; Brinker, U. H.; Mieusset, J.-L., Eds.; John Wiley & Sons: New York, 2010; pp 227−268.

(2) (a) Cram, D. J.; Tanner, M. E.; Thomas, R. *Angew. Chem., Int. Ed. Engl.* **1991**, *30*, 1024–1027. (b) Warmuth, R. *Angew. Chem., Int. Ed. Engl.* **1997**, *36*, 1347–1350. (c) Ziegler, M.; Brumaghim, J.; Raymond, K. *Angew. Chem., Int. Ed.* **2000**, *39*, 4119–4121. (d) Liu, X.; Chu, G.; Moss, R. A.; Sauers, R. R.; Warmuth, R. *Angew. Chem., Int. Ed.* **2005**, *44*, 1994–1997. (e) Warmuth, R.; Makowiec, S. *J. Am. Chem. Soc.* **2007**, *129*, 1233–1241.

(3) (a) Kang, J. M.; Santamaria, J.; Hilmersson, G.; Rebek, J. *J. Am. Chem. Soc.* **1998**, *120*, 7389–7390. (b) Yoshizawa, M.; Tamura, M.; Fujita, M. *Science* **2006**, *312*, 251–4. (c) Fiedler, D.; van Halbeek, H.; Bergman, R. G.; Raymond, K. N. *J. Am. Chem. Soc.* **2006**, *128*, 10240–10252. (d) Pluth, M. D.; Bergman, R. G.; Raymond, K. N. *Science* **2007**,

316, 85–88. (e) Hastings, C. J.; Pluth, M. D.; Bergman, R. G.; Raymond, K. N. *J. Am. Chem. Soc.* **2010**, *132*, 6938–6940.

(4) (a) Yoshizawa, M.; Takeyama, Y.; Kusukawa, T.; Fujita, M. *Angew. Chem., Int. Ed.* **2002**, *41*, 1347–9. (b) Chen, J.; Rebek, J., Jr. *Org. Lett.* **2002**, *4*, 327–329. (c) Warmuth, R.; Maverick, E. F.; Knobler, C. B.; Cram, D. J. *J. Org. Chem.* **2003**, *68*, 2077–2088. (d) Kaanumalle, L. S.; Gibb, C. L. D.; Gibb, B. C.; Ramamurthy, V. *J. Am. Chem. Soc.* **2005**, *127*, 3674–3675. (e) Gibb, C.; Sundaresan, L. D.; Kumar, A.; Ramamurthy, V.; Gibb, B., C. *J. Am. Chem. Soc.* **2008**, *130*, 4069–80. (f) Murase, T.; Horiuchi, S.; Fujita, M. *J. Am. Chem. Soc.* **2010**, *132*, 2866–7.

(5) (a) Romanova, Z. S.; Deshayes, K.; Piotrowiak, P. *J. Am. Chem. Soc.* **2001**, *123*, 2444–2445. (b) Romanova, Z. S.; Deshayes, K.; Piotrowiak, P. *J. Am. Chem. Soc.* **2001**, *123*, 11029–11036.

(6) (a) Yoon, J.; Cram, D. J. *J. Am. Chem. Soc.* **1997**, *119*, 11796–11806. (b) Scarso, A.; Shivanyuk, A.; Hayashida, O.; Rebek, J., Jr. *J. Am. Chem. Soc.* **2003**, *125*, 6239–6243. (c) Xu, D.; Warmuth, R. *J. Am. Chem. Soc.* **2008**, *130*, 7520–7521.

(7) (a) MacGillivray, L. R.; Atwood, J. L. *Nature* **1997**, *389*, 469–472. (b) Rivera, J., M.; Martin, T.; Rebek, J., Jr. *Science* **1998**, *279*, 1021–1023. (c) Ziegler, M.; Davis, A. V.; Johnson, D. W.; Raymond, K. N. *Angew. Chem., Int. Ed.* **2003**, *42*, 665–668. (d) Seeber, G.; Tiedemann, B. E. F.; Raymond, K. N. *Top. Curr. Chem.* **2006**, *265*, 147–183.

(8) Chapman, R. G.; Sherman, J. C. *J. Am. Chem. Soc.* **1999**, *121*, 1962–1963.

(9) (a) Liu, X. J.; Liu, Y.; Li, G.; Warmuth, R. *Angew. Chem., Int. Ed.* **2006**, *45*, 901–904. (b) Liu, X. J.; Warmuth, R. *J. Am. Chem. Soc.* **2006**, *128*, 14120–14127.

(10) Helgeson, R. C.; Knobler, C. B.; Cram, D. J. *J. Am. Chem. Soc.* **1997**, *119*, 3229–3244.

(11) Rowan, S. J.; Cantrill, S. J.; Cousins, G. R. L.; Sanders, J. K. M.; Stoddart, J. F. *Angew. Chem., Int. Ed.* **2002**, *41*, 899–952.

(12) See Supporting Information (SI) for structure details.

(13) Addition of (*S*)-1-phenylethanol to the NMR sample led to the splitting of two imine signals (see SI).

(14) Bringmann, G.; Price Mortimer, A. J.; Keller, P. A.; Gresser, M. J.; Garner, J.; Breuning, M. *Angew. Chem., Int. Ed.* **2005**, *44*, 5384–5427.

(15) Chapman, R. G.; Sherman, J. C. *J. Org. Chem.* **2000**, *65*, 513–516.